Electroluminescent Organic and Quantum Dot LEDs: The State of the Art

Poopathy Kathirgamanathan, Lisa M. Bushby, Muttulingam Kumaraverl, Seenivasagam Ravichandran, and Sivagnanasundram Surendrakumar

***Abstract*—A detailed background into the reasons for the feverish interest and growing impact on commercial market share of organic light-emitting diode (OLED) technology for lighting and display applications is given. Following this, the increasing discussion over whether electroluminescent devices based on quantum dots will ever challenge that of organics in displays is considered. The unique physics and chemistry of quantum dots results in narrow emission bands and increased stability over organic dyes meaning the potential for this is significant. The current best efficiencies of quantum dot devices and associated device structures from the literature are presented followed by a comparison of devices fabricated with organic materials, in particular those of polymers, metal complexes (fluorescent and phosphorescent) and small molecules.**

***Index Terms*—Inorganic light-emitting diodes, organic light-emitting diodes (OLEDs), quantum dots.**

I. Historic Development of Lighting Solutions

THE development of lighting solutions over the last 150 years has been driven by number of factors, namely lower cost, increased brightness, longer lifetime, and more efficient devices that use more environmentally-sustainable materials.

The tungsten light bulb was a revolutionary step up from candles and oil lamps. Owing to its effectiveness at filling rooms with white light at the flick of a switch, it quickly became the lighting solution of choice and became a fixture in almost all buildings with a source of electricity. But the tungsten lamp was not perfect; grossly inefficient it created significant excess heat. Nonetheless, its easy manufacturability and low cost meant it would be some time until its use began to be rivalled by the much more efficient compact fluorescent light bulb (CFL) (50–60 lm/W cf. 8–10 lm/W) that was introduced in the 1970s. Besides using less energy, CFLs also lasted much longer: in the region of 5000 hours cf. 800 hours. They have since become ubiquitous in households and commercial buildings as governments around the world introduced phase-out programs of traditional (so-called incandescent) bulbs in favor of newer generations of energy-efficient lighting. See Fig. 1.

Fig. 1. Historic development of more efficient lighting solutions.

Although more energy efficient, the CFL bulb has its own environmental concerns, containing as it does the hazardous substance mercury, which means a number of controls must be instituted during manufacture and disposal to prevent release into the environment and to protect human health. Parties and signatories to the UN's Minamata Convention on Mercury[1] have agreed to ban the production, export, and import of certain types of CFL by 2020 owing to their mercury content. As a result, the non-mercury-containing third generation of light bulb, the LED, which also provides further efficiency improvements (60–80 lm/W) over the CFL bulb has taken over significant swathes of market share and is continuing to do so.

LED light bulbs make use of the principle of electroluminescence (EL), although it is first appropriate to consider the mechanics of photoluminescence (PL) . PL is the term given to describe the radiative decay process in a material; it is a more general term than fluorescence or phosphorescence, which describe emission from specific states: either excited singlet or triplet states, respectively. For organic molecules, fluorescence usually occurs from the lowest vibrational level of the excited singlet state. It is a so-called spin-allowed transition, so it occurs quickly, typically on the nanosecond time scale. Phosphorescence, in contrast, occurs after intersystem crossing from an excited singlet state to an excited triplet state; and as this process is spin forbidden, it typically occurs over a longer period—in the microsecond to second time frame. The process is generally described figuratively using a Jablonski diagram that shows the absorption and deactivation processes of organic molecules (Fig. 2). Many heavy metals, such as transition metals (e.g., Ir, Pt) and lanthanide/rare earths are “phosphorescent” owing to spin-orbit coupling, which weakens the rules around spin allowed and spin forbidden transitions.

As can be seen in Fig. 2, the energy associated with emission is less than that of absorption (excitation) meaning that emitted photons have less energy than those that are absorbed and so

Manuscript received January 08, 2015; revised March 12, 2015; accepted March 19, 2015. Date of publication March 31, 2015; date of current version May 04, 2015.

The authors are with the Institute of Materials and Manufacturing, College of Engineering, Design and Physical Sciences, Wolfson Centre for Materials Processing, Brunel University London, Uxbridge, UB8 3PH, U.K. (e-mail: p.kathir@brunel.ac.uk).

Color versions of one or more of the figures are available online at http://ieeexplore.ieee.org.

Digital Object Identifier 10.1109/JDT.2015.2418279

[1]Minamata Convention on Mercury. [Online] Available: http://www.mercuryconvention.org

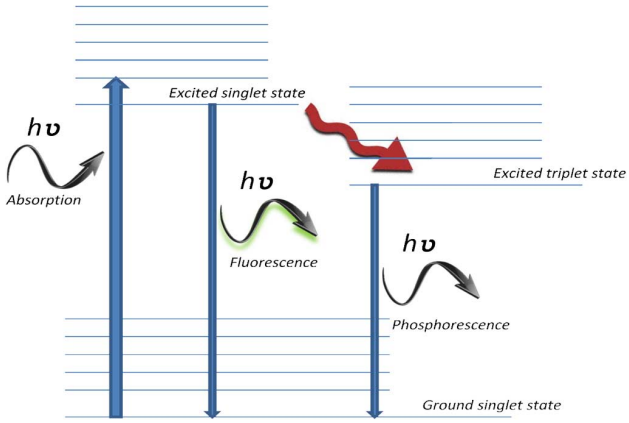

Fig. 2. Jablonski diagram showing absorption and emissive deactivation processes of organic molecules.

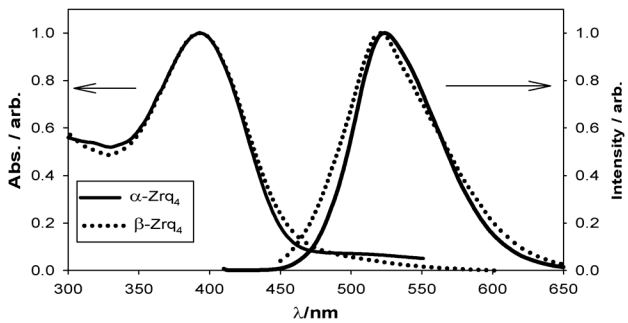

Fig. 3. Absorption and emission spectra of Zrq_3.

the spectra are shifted to longer wavelengths. In addition, as absorption can occur from any one of several vibrational energy levels in the ground state to any one of various excited vibrational states, absorption and emission spectra of typical organic molecules, which include the vibrational levels of many atoms, are characteristically broad. See Fig. 3.

Where the excited triplet state is long lived and close in energy to the excited singlet state, an additional mechanism for fluorescence may occur. Known as thermally activated delayed fluorescence (TADF), the singlet state is populated through: 1) excitation and 2) intersystem crossing then occurs to the triplet state. At this point, rather than the triplet relaxing back to the ground state: 3) a second intersystem crossing process back to the excited singlet occurs, from where: 4) fluorescence takes place, as shown in Fig. 4.

EL is the phenomenon whereby light is emitted from a material following the application of an electric field to it. The process can be described by an analogous mechanism to that of PL where rather than exciting the molecule through the absorption of radiation, the molecule is excited electrically. The molecule then relaxes to its ground state radiatively and EL results (Fig. 5).

The energy levels of organic molecules are often described as the lowest unoccupied molecular orbital (LUMO), or the excited state, and the highest occupied molecular orbital (HOMO), or the ground state, as can also be seen in Fig. 5, with the distance between the two levels the energy bandgap (Eg).

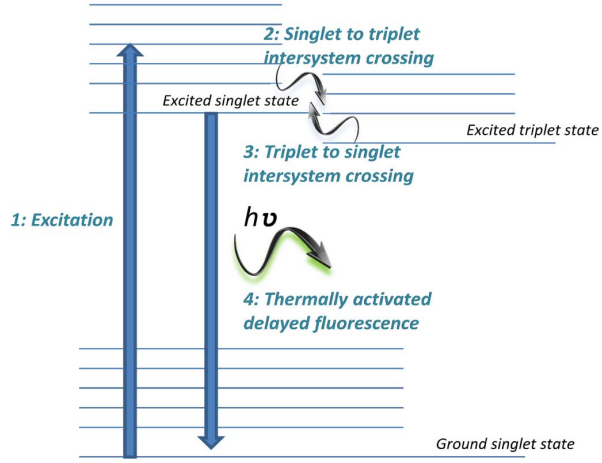

Fig. 4. Mechanism of thermally activated delayed fluorescence.

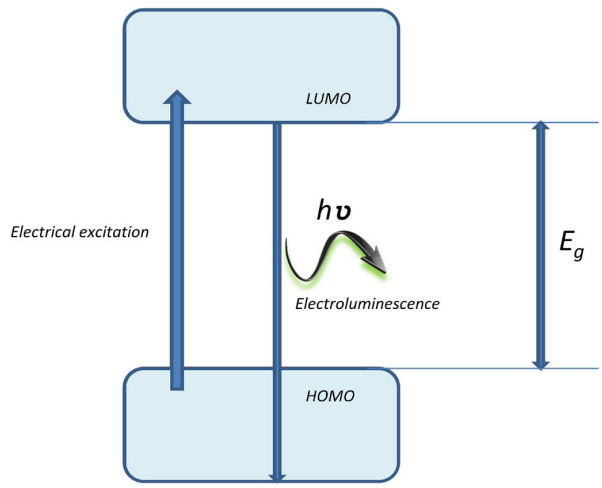

Fig. 5. Mechanics of electroluminescence in organic molecules.

Major breakthroughs in harnessing EL have been made possible through the development of wide bandgap light emitting diodes (LEDs) in the 1960s, the development of evaporated organic films in the 1980s and most recently through the development of solution-processable quantum dots.

One of the first observations of EL was in the 1930s by Destriau [1], who found that certain zinc sulphide phosphors could be excited by low voltage, low frequency alternating current. Crucially, no heat was emitted during the process creating the potential for highly-efficient lighting solutions. Destriau also discovered that doping ZnS with "activators" such as Mn^{2+}, Cu^{+} or Ag^{+}, could lead to enhanced emission, although charge compensation, i.e. the addition of "co-activators" such as Cl^{-}, Br^{-} or I^{-} is an important factor in this.

Between 1953–1955, Bernanose published details of one of the first observations of EL of organic compounds, namely acridine derivatives [2], [3], in which brightness vs applied field followed the same emission laws to those found for inorganic phosphors. In particular, Bernanose studied acridine orange on cellulose films from which EL was observed following the application of high alternating voltages. His studies found that the emission spectrum was independent of the applied field with the

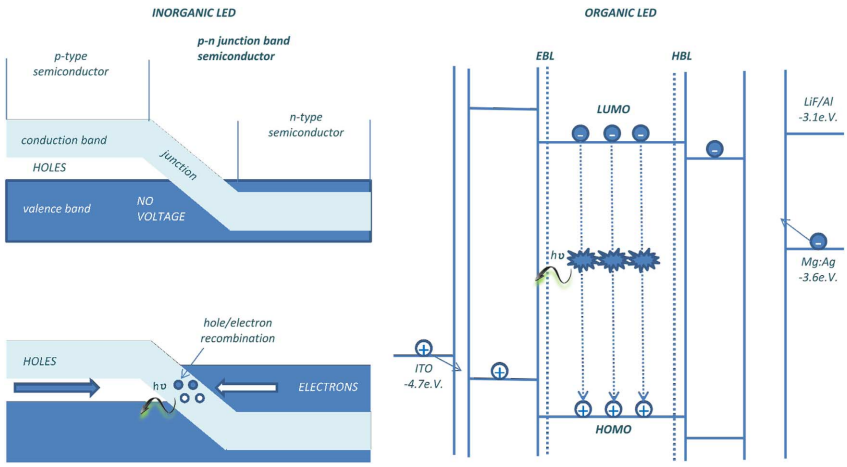

Fig. 6. Principle of electroluminescence in semiconducting (inorganic) and organic LEDs.

proposed mechanism being either direct excitation of the dye molecules or excitation of electrons.

The first observations of EL in organic materials proved problematic in terms of the potential for commercialization of the technology, however. For instance, in 1965, Helfrich and Schneider had to apply currents of 50–1000 V to anthracene crystals to observe fluorescence [4], and progress was further hampered by difficulties in crystal growth and short lifetimes. Around the same time, General Electric introduced the first commercial LEDs based on the inorganic semiconductor GaAsP [5]and over the next few decades, while research into organic EL waned, that related to inorganic LEDs flourished.

An inorganic (semiconductor) LED essentially consists of several layers including an n-type layer with a surplus of negative electrons and a p-type layer with an insufficient amount of electrons (also described as a layer with a surplus of positive holes). An active layer is sandwiched between them. When an electric voltage is applied, the electrons and holes flow towards the layer they are attracted to. Their paths cross in the active layer where they recombine radiatively and light is emitted. See Fig. 6.

A succession of LEDs based on III–V semiconductors, such as GaAs, GaP, AlGaAs, InGaP, AlInGaP, were all developed, but devices tended to be red, orange, green and yellow as the color of the emission is based on the energy gap of the semiconducting material, and blue-colored devices remained elusive. It was some time before blue diodes based on materials such as ZnSe or GaN were developed and these still exhibited significantly lower efficiencies than other diodes [6]. It was for the blue emitting GaN-based device that The Nobel Prize in Physics 2014 was awarded. p-i-n junction inorganic LEDs offer long lasting and more efficient alternatives to older lighting technologies.

II. Multi-Color Display Technologies

Traditional technologies for multi-color displays utilizing cathode ray tubes (CRT) or liquid crystal displays (LCD) have significant limitations that prohibit their use in one way or another. CRTs, for example, have a much higher power usage than LCDs and require bulky devices. In the case of LCDs, a white light source is used as the backlight and a liquid crystal, that can filter the white light to a variable degree, is placed in front of each subpixel in a device. The "filter" allows a range of wavelengths appropriate to its color through at any one time thus creating the multi-color capability. The brightness of the subpixel is controllable as the liquid crystal is energized or not to block or transmit light. It is the crystal filtering mechanism that causes poor viewing angles on LCD displays.

It is possible to use LEDs as the white light source in LCD displays and these tend to produce better contrast and color coordinates than fluorescent backlights. Plasma displays are generally not as efficient as so-called LED-LCDs.

In the first instance, LED technology would seem to tick many of the boxes required for display applications. ZnS and SrS are among the most common phosphor materials used in thin-film electroluminescent (TFEL) displays, although to obtain EL, the phosphor must be intentionally doped with either transition metal [7]or lanthanide luminescent impurities [8]. Expanding the applicability of semiconductor materials beyond lighting and backlighting solutions continues to pose significant challenges owing to the difficulties with the requirement to display more than one color.

Under active-matrix conditions, multi-color LEDs can be assembled into an EL display as demonstrated by Barrow and Tuenge of Planar Systems, Inc. [9]in a prototype multi-color display using ZnS:Mn and ZnS:Tb phophor layers. EL subpixels can be arranged in two-dimensional arrays each with its own row and column address and associated data value. To make a full color display, one or more subpixels of different colors are grouped together to form a pixel. Thus each pixel on an EL display includes one or more subpixels, e.g. red, green and blue.

More than 30+ years on, however, full-color TFEL displays based on semiconductors are generally only available in small format active matrix design as cost-effective full-color panels remain problematic to commercialize and the devices are still only used in backlighting applications.

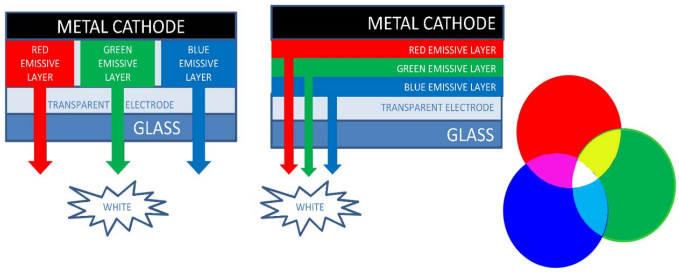

Fig. 7. Multi-color OLED devices and the ability to generate white light.

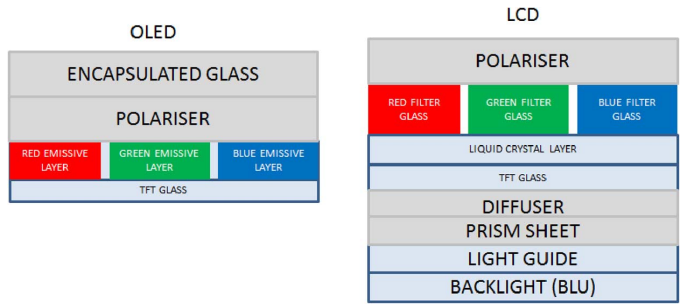

Fig. 8. Simplicity of OLED design vs LEDs.

III. Introducing OLED Technology to the Market: Two Aspects—Lighting and Displays

Interest in organic EL was revived when Tang and VanSlyke fabricated devices using thin evaporated films (∼100 nm) of aluminum 8-hydroxyquinoline (Alq_3) and low voltages (∼10 V) [10]. This breakthrough development made it clear that, given improvements in efficiency and reliability, it would be possible to manufacture low-cost, flexible, multi-color and white displays based on organic EL. Further attention was drawn to this possibility with the advent of similar devices fabricated by Burroughes *et al.* [11] based on the conjugated polymer polyparaphenylenevinylene (PPV) which could be formed via the low-cost route of spin casting from solution and subsequent thermal treatment. The development of a solution-processable precursor for PPV and poly(fluorenes) made this a potentially attractive approach for simple light-emitting diode fabrication.

OLEDs rely on a central layer of emissive organic material that is electroluminescent, that is, it will emit light when excited by an electrical current. Electrons are injected from the cathode and holes from the anode. These travel inwards into the device where they recombine to form excitons in a singlet:triplet ratio of 1:3. The spin-allowed emission from fluorescent excitons may occur rapidly, otherwise the normally non-radiative triplet excitons may emit if the active layer is phosphorescent. As there are often difficulties in injecting electrons and holes (carriers) into the organic layer, the structure of an OLED usually includes additional layers, such as electron injecting and transporting layers and hole injection and transport layers to facilitate the injection of charge carriers. The layers are deposited on top of each other with the first deposited on a substrate (Fig. 7). The anode must be transparent to allow the photons produced to be seen, and so it is usually transparent ITO, although it could equally be polyethyleneterephathalate (PET) coated with a transparent conductor for a flexible device or any other transparent material.

Devices are typically assessed through a number of characterization measurements that include color coordinates (perceived color), current density (A/cm^2) versus voltage, luminance (a measure of brightness in cd/m^2) versus voltage, current efficiency (cd/A) versus luminance, power efficiency (lm/W) versus luminance and lifetime (a measure of the stability of the device).

Critically, the incremental cost and ease of producing multi-color devices over single color or white devices is negligible as the fabrication technique of making a multi-color device simply involves the deposition of additional layers of emissive material onto the same substrate (Fig. 8).

Fig. 9. Selected commercial OLED displays.

The inclusion of polymers and organic molecules as emissive layers in devices of various structures have been the subject of many thousand research papers and patent applications since the 1980s each demonstrating an improvement in efficiency, color coordinates, lifetime or brightness over the last, with the result that the efficiencies of the devices and thus the commercial viability of the technology improved exponentially.

OLEDs are now a commercial reality in many display applications (Fig. 9) and it is worthy of note that as they can be deposited onto virtually any substrate, e.g. glass, ceramic, metal or plastic. It is also possible to manufacture flexible or curved devices, which is not the case with semiconducting LEDs, LCDs or plasma technologies.

In addition to use in displays, OLEDs have the potential to be used in lighting applications.

A key advantage of using an OLED light over an LED light source is its favorable color rendering properties as given by its color rendering index (CRI). The CRI has been defined the International Commission of Illumination (CIE) as the effect of an illuminant on the color appearance of objects by conscious or subconscious comparison with their color appearance under a reference illuminant. Effectively, it is the quantitative measure of the ability of a light source to reveal the colors of objects in comparison with a natural light source.

Semiconductor LED light bulbs have struggled to reach the more desirable warmer whites with values of 80–85 compared to the highest CRI achievable of 100 for a black body radiator.

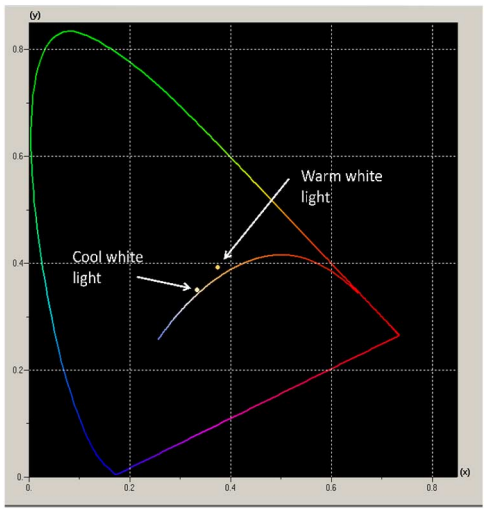

Fig. 10. CIE color coordinate chart showing warm and cool warm light.

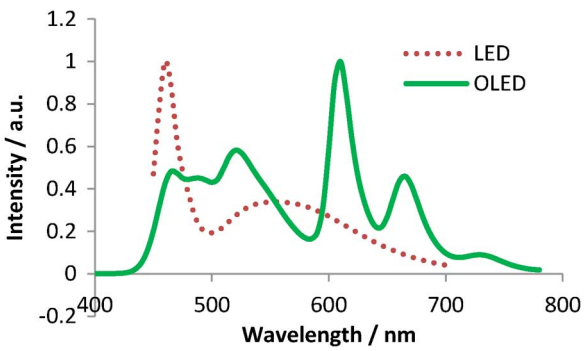

Fig. 11. White OLED vs white LED emission spectra.

OLEDs can get much closer values of 90–95 to the ideal. The CIE chart showing the relative positions of warm and cool light is given in Fig. 10 and a typical emission spectra of a white OLED and white LED is given in Fig. 11 where the significant emission in the blue region of the spectrum can clearly be seen for the LED.

While technology into OLED lighting and research is somewhat in its infancy, the same kind of improvements that were seen in OLED displays enabling commercial devices over the last few years are expected in lighting solutions in the next 3+ years. For example, in 2009, Matsushita (National Panasonic) Electric Works demonstrated a WOLED with an efficiency of 37 lm/W with a lifetime in excess of 10000 hours at an initial luminance of 1000 cdm^{-2} and improved it to 150 lm/W with a lifetime in excess of 20,000 hours at 3000 cdm^{-2} in 2014 [12]. In addition to Matsushita, there are a number of large companies heavily involved in OLED lighting, such as Samsung, LG, Pioneer, Hitachi, Osram, Philips, GE, and BOE.

The market for both OLED lighting and displays has grown steeply since 2000, with the market, particularly for OLED lighting, predicted by IDTechEx to continue to show strong growth through 2018 and beyond (Fig. 12).

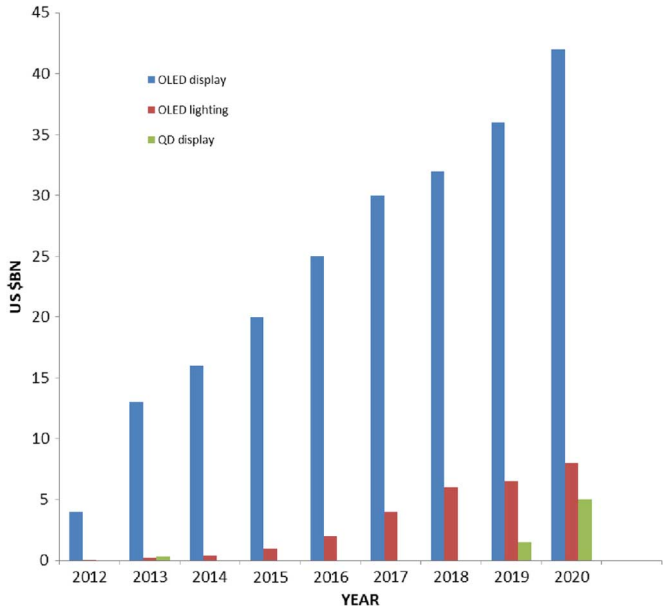

Fig. 12. Projected market for OLED lighting, QDs and displays [IDtechEX, Santa Clara, November 2014].

IV. Quantum Dots

Quantum dots (QDs) have become the subject of intense academic and industrial (Nanoco, QD Vision, Nanosys, Samsung, Dow Chemicals) research over the past 15 years owing to their novel electronic, electrical, optical and catalytic properties with wide ranging applications in displays, lighting, lasers, solar cells and photoelectrochemical cells.

Quantum dots are nanocrystals composed of III–V semiconductor (e.g. GaN, GaP, GaAs, InP and InAs) and II-VI semiconductor (e.g. ZnO, ZnS, CdS, CdSe, and CdTe) materials with all three dimensions in the approximately 1–10 nm size range. Among these, CdSe/ZnS systems have been studied most as far as the EL is concerned, although, Cd is environmentally restricted owing to its toxicological properties and its viability as a commercial material is consequently questionable.

It is the size of the QD that imparts unique physical properties on the material: in contrast to the bulk semiconductor, the electrons in a nanocrystal exhibit quantum mechanical effects. The so-called quantum confinement phenomenon occurs as the size of the semiconductor becomes comparable to or smaller than the exciton Bohr radius, and where the electron and hole are confined by the boundaries of the material. It leads to discrete energy levels, known as "confinement states", as predicted by a particle in a box (Schrödinger's) equation [see (1)].

$$E = \frac{n^2 h^2}{8mL^2} \tag{1}$$

where n is the quantum number; h is Planck's constant; m is the electronic mass, and L is the width of the box.

These levels correspond to bonding (HOMO) and anti-bonding (LUMO) levels in the material (Fig. 13). While bulk semiconductors have a set bandgap (Eg) between the valence and conduction bands, an effect of quantum confinement means that the bandgap energy of a QD is inversely proportional to its size (smaller QDs emit higher energy than

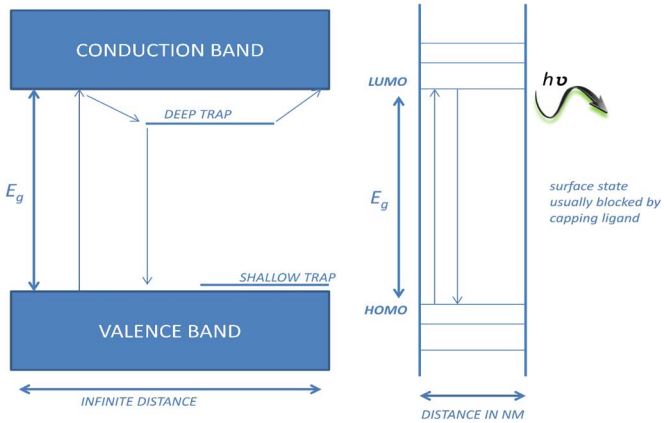

Fig. 13. Energy bandgaps of bulk semiconductor and QD materials.

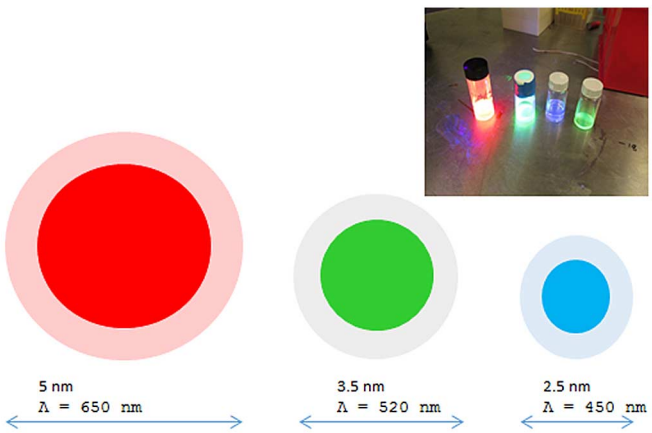

Fig. 14. Top image of PL of selected quantum dots in hexane [QD source: Sigma Aldrich]. Schematic of tunability of QDs—effect of size distribution on color of PL emission below.

larger QDs), and this means that the emission from a QD is color tunable (Fig. 14).

Although radiative, a QD that comprises of a single semiconducting material generally exhibits low quantum efficiencies owing to non-radiative electron-hole recombinations that occur at defects in the crystal and dangling bonds on the surface. For example, Xie *et al.* [13] found that after 12 hours in air, the absorption spectrum of an InP QD sample shifted to the blue dramatically, which was attributed to the fast shrinkage of the inorganic core by oxidation. As a result, shell materials, typically with wider bandgap energies, such as CdS or ZnS are grown on the surface of the core [14] in a process known as inorganic passivation. Confining charge carriers within the luminescent core and away from the surface significantly reduces the effects of surface defects caused by atoms on the surface of the crystal. In this way, states that may function as centers for non-radiative recombination are protected and there is a consequent increase in photoluminescent quantum yield (PL QY).

Xie found that after growing a ZnS shell around the InP core, the absorption properties of the nanocrystal were unchanged following exposure to air, indicating a much improved stability. Further, they found that the PL QY of the InP dot was low ($<1\%$), but that it reached $>40\%$ for the core/shell ones.

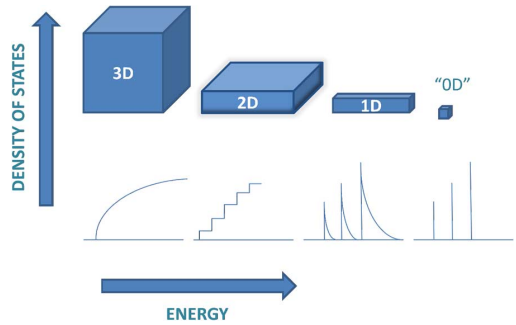

Fig. 15. Cluster diameter versus energy gap.

QDs absorb all wavelengths higher in energy than their bandgap and convert them into a single color, i.e. they have broad absorption spectra, but narrow emission spectra. This feature gives them advantages over organic fluorophores because the excitation wavelength can be anywhere within a broad range [15]. The narrow emission spectra of QDs and the tunability of such results in an extremely wide color gamut, and thus QD displays have the potential for improved color saturation over OLED displays.

QLEDs are also solution processable (low cost) and have theoretical performance limits that meet or exceed that of all other display technologies [16]. As both the color coordinates and luminous efficiencies of QLEDs are good they are therefore capable of being more power efficient. Furthermore, as with OLED displays, they can be deposited on any substrate enabling many exciting possibilities in terms of shape and design. It is well-known that the absorption spectrum shifts to red as the size of the nanocrystal increases. Typical emission spectra show a full-width at half maximum (FWHM) of 30–40 nm depending on the degree of monodispersity achieved during synthesis [17]. QDs can be both electrically and optically excited, where internal EL quantum efficiencies as high as 90% have been obtained for certain materials [18].

Owing to colloidal stability and the ability to make thin films without disrupting the physical integrity of the crystal, the use of QDs in flexible EL displays becomes a possibility. Further, solution processing enables low cost full color display manufacturing, e.g., using spin processing [19] or inkjet printing [20] techniques. Such techniques can be applied to additive processing, such as vacuum deposition [21], and hence are more affordable methods for display fabrication. The bandgap is also dependent on the cluster diameter, and this also affects the distribution of spectral emission, i.e. the smaller the cluster, the narrower the emission band. See Fig. 15.

QDs are generally prepared by reacting inorganic precursors in the presence of organic ligands, which eventually form a molecular coating around the QD luminescent core and stabilise the nanoparticles against aggregation (Fig. 16).

Factors that are important to optimize during inorganic passivation include the energy levels of the shell and core, the formation of a defect-free and uniform coating, coherence strain between with the shell and core lattice, and the thickness of the shell layer. The maximum PL efficiency of the core/shell QD is dependent on the thickness of the shell layer, which has

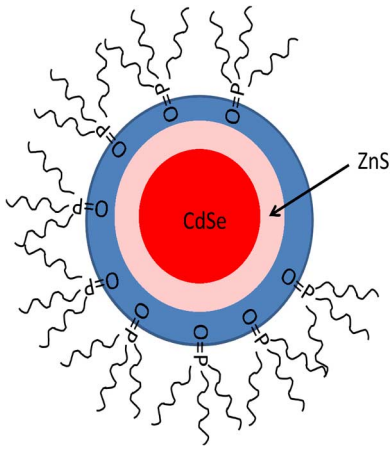

Fig. 16. Example of a passivated core-shell quantum dot structure.

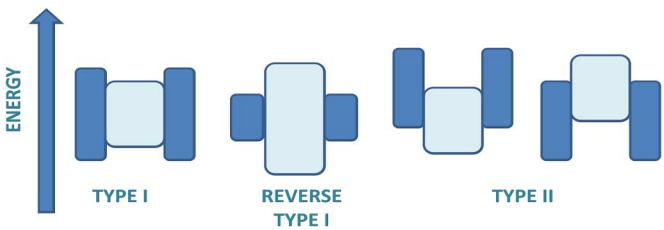

Fig. 17. Energy bandgaps in Type I, Reverse Type I and Type II QDs.

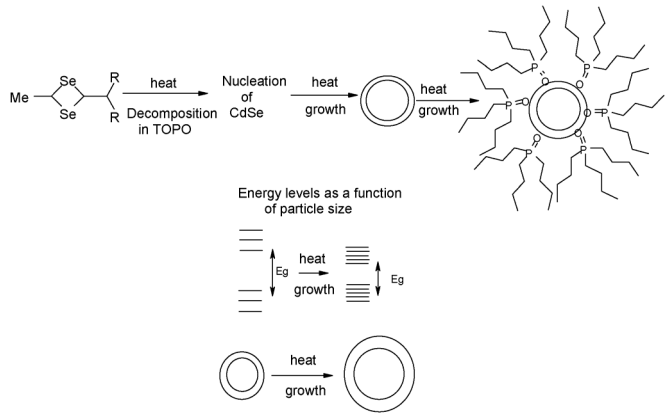

Theoretical decomposition schematic for the preparation of TOPO capped CdSe using a single source precursor

Fig. 18. Typical synthetic route developed by Ludolph *et al* for the preparation of TOPO-capped CdSe using a simple precursor [26].

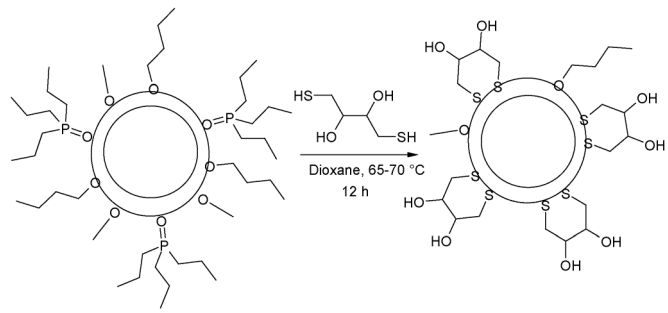

Fig. 19. Schematic of capping ligand replacement mechanism.

been found to be less than two monolayers thickness for optimum properties of a CdSe/CdS core/shell structured nanoparticle. Thicker capping layers lead to the formation of misfit dislocations, which are also sites of non-radiative recombination, leading to a decrease in the PL QY [22].

The quantum efficiency of the QD will be further increased by a defect-free, and uniform shell coating to minimize the number of non-radiative recombination sites within the QD. Further, when the shell material coats the core surface the bonding lattice, lattice parameters, such as coherency strains result and can play an important role in the properties of these core/shell systems. For instance, strain may cause the absorption and emission spectra of core/shell QDs to be red shifted [23].

Depending on the bandgaps and the relative position of the electronic levels of the involved semiconductors, the shell can have different functions in core/shell QDs. Fig. 17 gives an overview of the band alignment of the bulk materials where three types can be distinguished: Type I where the bandgap of the shell is larger than that of the core, Reverse Type I where the bandgap of the shell is smaller than that of the core and Type II where either the valence band edge or the conduction band edge of the shell material is located in the bandgap of the core.

It is crucial to match the energy levels of the shell and core. For Type I QDs, passivation of the QD surface should be with a material that has a larger bandgap energy to increase the efficiency of charge injection into the radiative core. A wider bandgap shell material is desired to create a potential barrier around the QD core to confine the excitons. Confinement of charge carriers in the core region by the band offset potentials results in efficient and photostable luminescence from QDs.

The surface of the core/shell QD may still possess highly reactive dangling bonds, and these can be used to further passivate the nanocrystal from its surrounding environment through the co-ordination of an organic ligand, such as tri-n-octylphosphine oxide (TOPO), trioctylphosphine (TOP), thiols (e.g. β-mercaptoethanol), carboxylic acids (e.g. oleic acids), octadecene, oleylamine or 3-(aminopropyl)trimethoxysilane (APTMS). The ligand chelates to the surface of the QD by donating lone pair electrons to the surface metal atoms, resulting in a QD that demonstrates reduced particle agglomeration, reduced sensitivity to oxidation, improved electronic stability and may be soluble in relatively non-polar media [24]. It also stabilises the nanocrystals to the extent that it possible to extract them as free-standing powders [25].

Ludolph *et al.* [26] has pioneered a route of synthesis for the preparation of a TOPO (tri-n-octylphosphine oxide) capped device, as shown in Fig. 18.

Organically-capped QDs may be photostable as the interface between the capping molecules and surface atoms is generally weak leading to the failure of passivation and the creation of new surface states under UV radiation. Surface modification by ligand replacement is possible to tailor the properties of the QD to the use for which it is required, for example it can be made hydrophobic or hyrophilic. Ligand replacement can be carried by reacting with an excess of another ligand or a ligand that has a higher complexing ability (high formation constant), for example a bidentate ligand (thiols), as shown in Fig. 19.

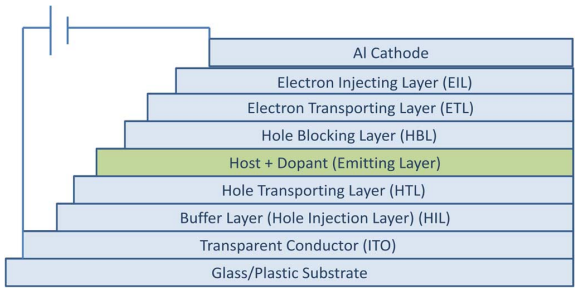

Fig. 20. Conventional OLED device structure.

Further, QDs can be anchored by polymers (in particular light-emitting polymers) by producing a monomer with a phosphonyl group, carrying out the QD synthesis in this medium and reacting the product with a polymerizable group (e.g., phenylvinylene) [27].

This ability for solution-based synthesis enables effective control of the crystal size distribution. The phenomena of "Ostwald ripening" is utilized whereby the higher free energy of smaller QDs makes them lose mass to larger size QDs, eventually disappearing. Using a co-ordinating solvent, such as TOPO, stabilizes the QD dispersion, improves the passivation of the surface and provides a steric barrier to slow the growth of the QD. The final size of the QD is mainly controlled by the reaction time and the temperature. As crystal size is directly correlated to the HOMO-LUMO bandgap of the material, it is possible to take aliquots during the reaction process, and observe the corresponding absorption wavelength shift to stop the reaction when the appropriate size of crystal is achieved. This method has been used extensively to synthesize II-VI and III-V QDs [28]. The method provides sufficient thermal energy to anneal defects resulting a monodispersed solution of QD. A typical standard deviation of particle size of 5% is achieved.

V. OLED and QLED Devices

The basic structure of an OLED consists of one or more organic films deposited between two electrodes, one of which is transparent (Fig. 20). Under electrical bias, electrons are injected from the cathode and holes from the anode into the organic material where they travel in the applied field until they meet and form an excited state that leads to radiative emission.

Devices fabricated using films that are deposited by sublimation under vacuum are more costly than devices fabricated with films that are deposited from solution, e.g., by spin casting. Film thicknesses range from 10 to 100 nm. The emissive layer should have a high quantum yield and be an effective charge transporter. Additional layers are usually added between the anode/cathode and organic layer as hole or electron transporting aids. Considering the energy alignment of the ground and excited electronic states of the emissive monolayers and the surrounding organic thin films is critical to the fabrication of an efficient device in order to reduce the energy level barriers between layers, i.e. the ETL and HTL should be optimized as a well charge balanced device will have higher efficiency [29]. Fig. 21 shows energy levels of some common hole and electron

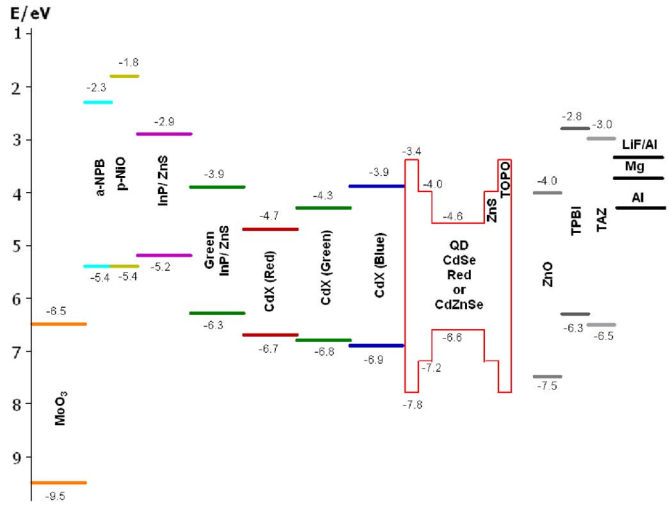

Fig. 21. HOMO-LUMO levels of selected QD materials and hole and electron transporting materials.

TABLE I
HOMO-LUMO Levels of Typical QDs

QD type	Color	HOMO (e.V.)	LUMO (e.V.)
CdSe/ZnS	Green	6.8	4.3
CdSe/ZnS	Red	6.7	4.7
InP/ZnS	Red	5.2	2.2

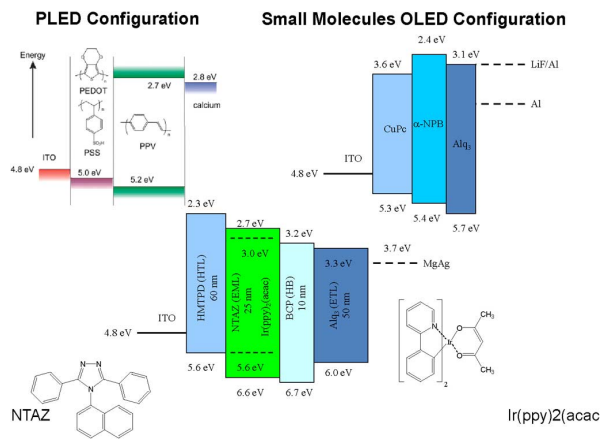

Fig. 22. Example OLED emissive layers with HTL/ETL energy levels.

transport materials used in OLEDs and HOMO-LUMO levels of typical QDs are shown in Table I.

In addition to QLEDs, we consider three types of OLED (Fig. 22), i.e. those where the emissive layer is based on polymers (PLED), fluorescent small molecules (e.g., Alq_3, OLEDs) or organo–metallic phosphorescent small molecules (e.g., $Ir(ppy)_3$, $Ir(ppy)_2(acac)$, PHOLEDs).

External quantum efficiency (EQE) can be expressed in analogous manner to that of an OLED by a well understood multiplication of four factors as described by (2)

$$\text{External quantum efficiency}(\eta_{\text{EQE}}) = \gamma\ \chi \cdot \eta_{\text{PL}}\eta_{\text{oc}} \quad (2)$$

where

γ = recombination efficiency of holes and electrons;
χ = fraction of charge carrier recombination in the emissive layer resulting in excitons with spin-allowed optical transitions;
η_{PL} = photoluminescent efficiency of the emitter;
η_{oc} = fraction of emitted photons that are coupled out of the device $(1/2n^2)$;
n = refractive index of the substrate (glass).

Of the different types of emissive layer in OLEDs, typically small molecules, e.g., Alq_3 have been shown to demonstrate good device lifetimes owing to the enhanced inherent stability of the molecules over phosphorescent materials, e.g. $Ir(ppy)_3$, phosphors offer high efficiency along with high internal quantum efficiencies, and polymer materials, e.g., PPV, have the advantage of being solution processable, but have lower EL efficiency.

Owing to the multiplicity of the excited states formed when the charges meet in the active layer of an OLED, around 25% of excitons are generated in the singlet state, with three times more triplet excitons (approximately 75%) being formed. This means that OLEDs based on fluorescent molecules have a maximum internal efficiency of around 25%. The efficiency of OLEDs can be dramatically improved by using phosphors, such as organometallic complexes with iridium or platinum metal ions that enhance spin-orbit coupling and enable emission from the formally forbidden triplet state. Phosphorescent OLEDs consequently have theoretical maximum internal efficiencies of 100% as in addition to the 75% of triplet excitons generated, relaxation of spin-orbit coupling rules means that the singlets that are also generated may be converted to triplets through intersystem crossing.

Recent OLED activity utilizes thermally activated delayed fluorescence (TADF), or upconversion to achieve near unity internal EL quantum yields from fluorphors by backfilling the singlet state with triplet excitons (T1 $\rightarrow$ S1 reverse intersystem crossing). The mechanism is described in Fig. 4, earlier. The need for more costly phosphorescent materials is eliminated, and the possibility of obtaining blue emitters that give very high total singlet yields [30], [31], is introduced. Indeed, Uoyama *et al.* [32] have reported OLEDs using EL metal-free molecules in which the energy gap between the singlet and triplet state is minimized by design allowing upconversion of excitons from the non-radiative triplet to the radiative singlet state thereby achieving efficiencies comparable to those in phosphorescence-based OLEDs. Green, orange and sky-blue OLEDs were fabricated with external EL quantum efficiencies of 19.3±1.5% (equivalent to 64.3%–96.5% internal efficiency), 11.2±1% and 8.0±1%, respectively.

Strong intermolecular interactions usually result in the low solubility of organic molecules, further they tend to form crystalline domains in the film state, which can act as carrier traps and raise the operational voltage of a device. As such, organic molecules in OLEDs are usually deposited onto a device by sublimation under vacuum, a costly technique, but polymer OLED materials are readily soluble in ink solvents meaning they can be wet processed into devices such as by inkjet printing or die coating much more cost effectively.

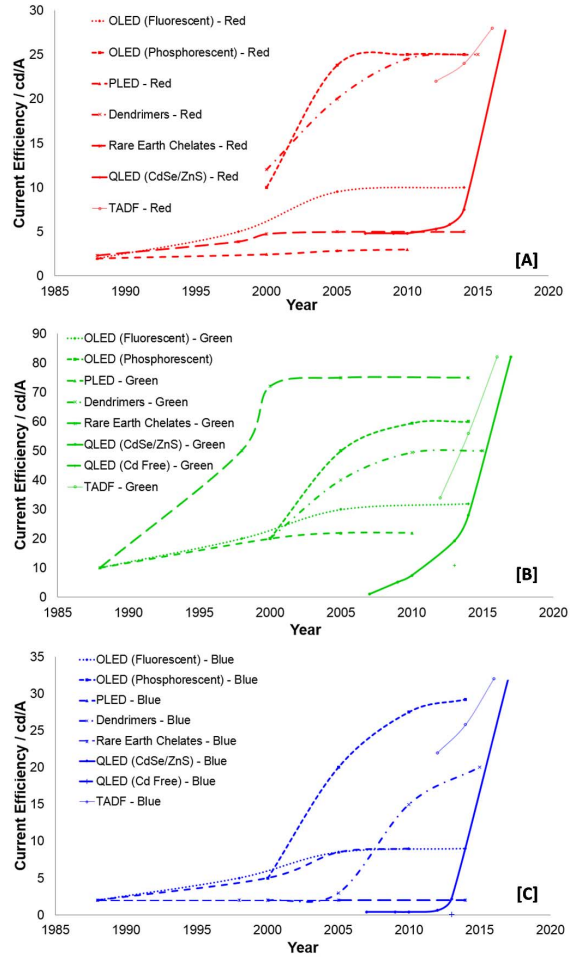

Fig. 23. Historic current efficiency data for OLED and QLED red [A], green [B], and blue [C] devices.

Blue colored OLED devices remain a key challenge. Compared to red (initial luminance 1000 cdm^{-2}, 500,000 hours) and green (initial luminance 1000 cdm^{-2}, 200,000 hours, according to Universal Displays at the OLED Summit 2013), the blue devices typically have lifetimes in the range 10,000–20,000 hours). Color coordinates of fluorescent blue OLEDs (0.15, 0.15) are considered acceptable with lifetimes of 50,000 hours at 1000 cdm^{-2} reported by Idemitsu Kosan and Merck. Blue phosphorescent OLEDs have poorer color coordinates of (0.20, 0.35) with a reported lifetime of 8000 hours at initial 1000 $\mathrm{cd/m}^2$. Printed PHOLEDs have even poorer lifetimes [33].

A further point of note is that OLEDs based on organic molecules have been found to degrade with time during prolonged excitation in a process known as photobleaching. Owing to the luminescent core being inorganic, which is then passivated by a protective inorganic shell, QDs are often much more resistant to photobleaching than organic dyes [34].

Despite high theoretical performance levels of QLEDs in practice, thus far efficiencies still lag behind those for OLEDs, but as can be seen in Fig. 23, there is a marked general trend

TABLE II
SELECTED TYPICAL PERFORMANCE DATA OF OLED AND QLEDS AT 1000 CDM^{-2}

COLOR	Fluorescent molecules	Phosphorescent molecules	Polymers/Dendrimers	Quantum dots
Red	(0.65, 0.35), 300-500 kh, 10 cd/A	(0.64, 0.36), 330 kh, 30 cd/A, 22 lm/W	(0.63, 0.37), 350 kh, 30 cd/A	
Red		(0.69, 0.31), 250 kh, 17 cd/A, 10 lm/W	(0.67, 0.32), 200 kh, 11 cd/A	(0.69, 0.31), 200 h, 15-20 cd/A, 15 lm/W
Green	(0.29, 0.61), 65 kh, 31 cd/A	(0.34, 0.62), 400 kh, 78 cd/A, 50 lm/W	(0.30, 0.63), 140 kh, 50 cd/A	(0.30, 0.68), 10 h, 12-35 cd/A, 10 lm/W
Blue	(0.15, 0.14), 50 kh, 10 cd/A, 5 lm/W	(0.18, 0.40), 20 kh, 50 cd/A, 30 lm/W	(0.15, 0.14), 20 kh, 6 cd/A	(0.16, 0.05), 1 h, 0.55 cd/A, 0.26 lm/W

Data given in the order: 1) CIE color coordinates (x,y); 2) lifetime; 3) current efficiency; 4) power efficiency

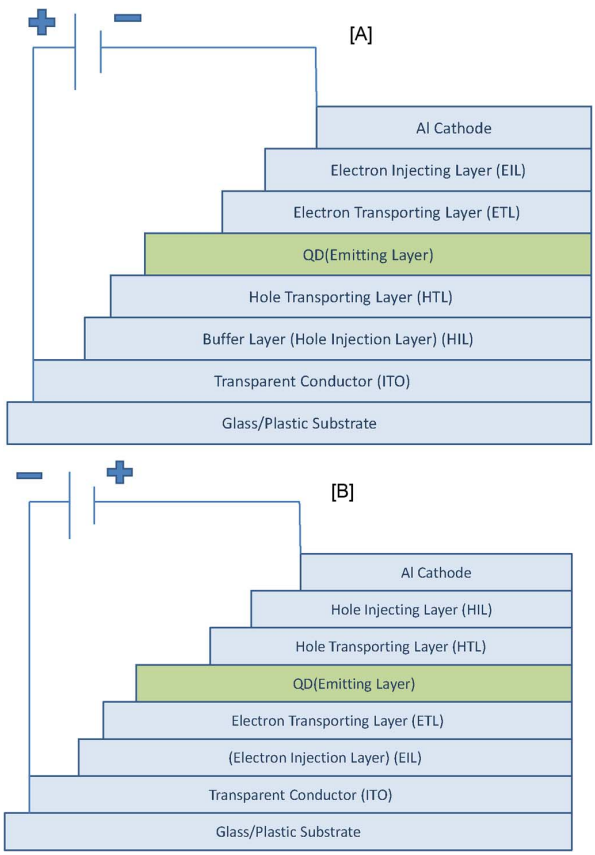

Fig. 24. Conventional [A] and inverted [B] QLED device structures.

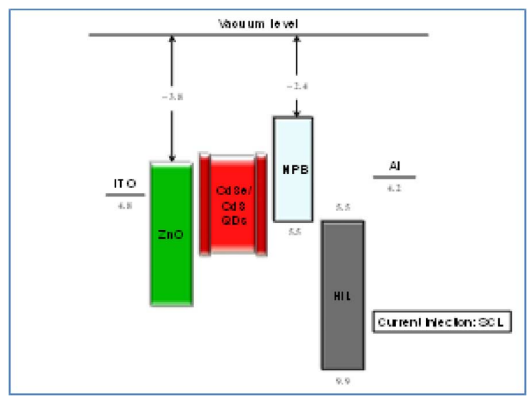

Fig. 25. Mashford *et al.* red device structure adapted from [35].

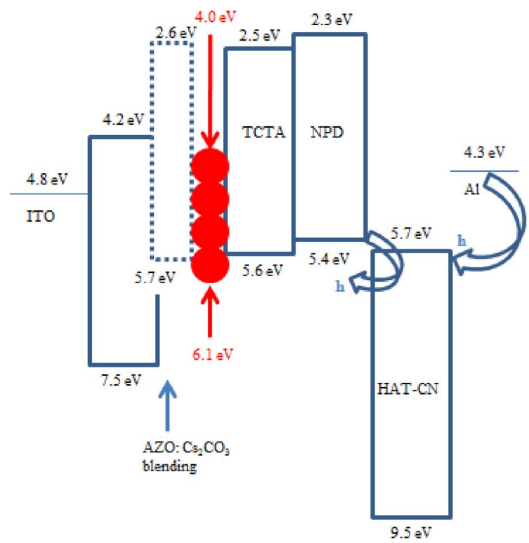

Fig. 26. Red device structure adapted from Kim and Jang [36].

towards improved efficiencies for red, green and blue devices, both OLEDs and QLEDs.

A comparison of typical device performance data based on fluorescent, phosphorescent, polymer and QD emissive layers at 1000 cdm^{-2} is given in Table II. It demonstrates that the performance of QD devices still lag behind those of OLEDs and that progress on blue devices across the board is still required.

QD device structures are largely similar to those of OLEDs (Fig. 24).

It is frequently found that in the literature on QLED and OLED devices that not all the relevant data (EQE, power efficiency, CIE co-ordinates and device lifetime) are reported for each device. While the PL efficiencies of QDs are high, the main reason for low EQEs in devices is largely attributed to poor charge carrier injection into the QD layers. Mashford *et al.*[35] has reported a red QD (CdSe/CdS) device that reaches a peak efficiency of 19 cd/A and 25 lm/W with an optimum thickness of 45 nm of QD and 0.68, 0.31 CIE coordinates. The lifetime was estimated to be 4 hours at 1000 cdm^{-2}. The device configuration is shown in Fig. 25.

Kim and Jang [14], [36] presented devices using CdSe/CdS/ZnS. Their red device achieved 6.5 cd/A and CIE (x,y)-coordinates of (0.70, 0.30), with a device structure shown in Fig. 26 and their green device an impressive 28 cd/A (0.16, 0.75), structure in Fig. 27. The lifetime was not reported.

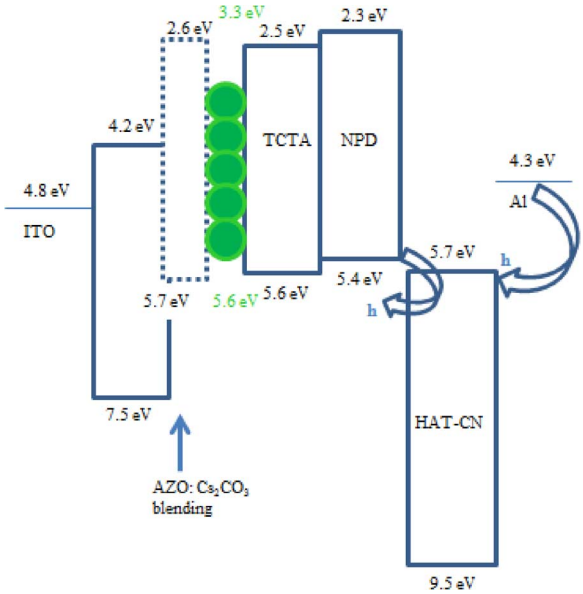

Fig. 27. Green device structure adapted from Kim and Jang [36].

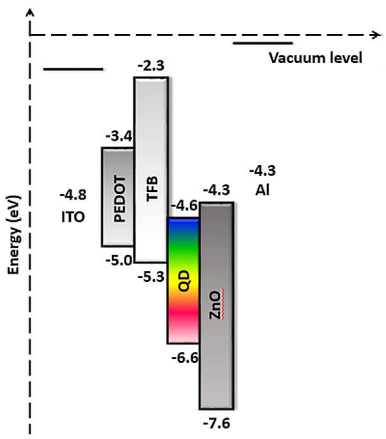

Fig. 28. Yellow device structure adapted from Qasim *et al.* [37].

A yellow device has been reported by Qasim *et al.* [37] that achieves 1.6 cd/A with peak EL emission at 575 nm. Again, lifetime data is not given. The device structure is given in Fig. 28.

These devices show the potential of QDs in devices for display applications, but their commercial viability is negligible owing to their reliance on the highly toxic and environmentally restricted Cd. As a result, efforts are now beginning to shift towards Cd-free device structures. While Lim *et al.* [38] presented results from a Cd-free QD in 2011 using InP, the efficiency was poor at 0.006 cd/A (Fig. 29). Two years later, his group reported a 10.9 cd/A green device [39] that was also cadmium free. (Fig. 30).

Kwak *et al.*[40] has reported bright and efficient inverted structure red, green and blue QLEDs with maximum luminances of 23,040, 218,800 and 2250 cd/m^2 and external quantum efficiencies of 7.3%, 5.8%, and 1.7%, respectively. The devices showed turn-on voltages as low as the bandgap energy of each QD and long operational lifetime, which they attributed to direct exciton recombination within QDs through the inverted device structure. In their device, the electrons were injected from the

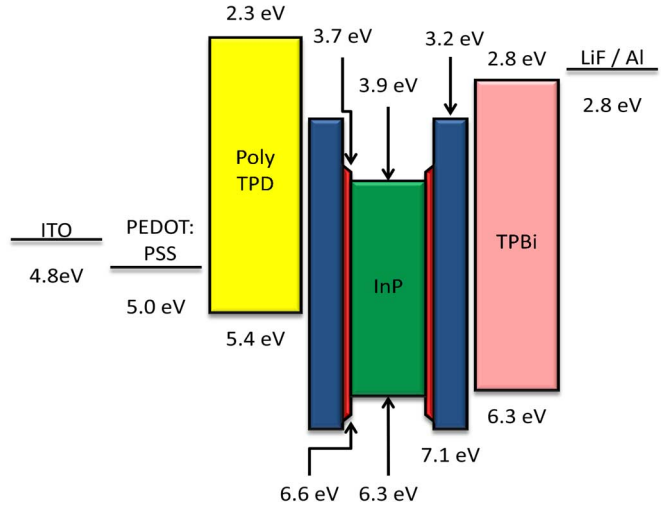

Fig. 29. Cd-free device structure (2011). (Lim *et al.* [32])

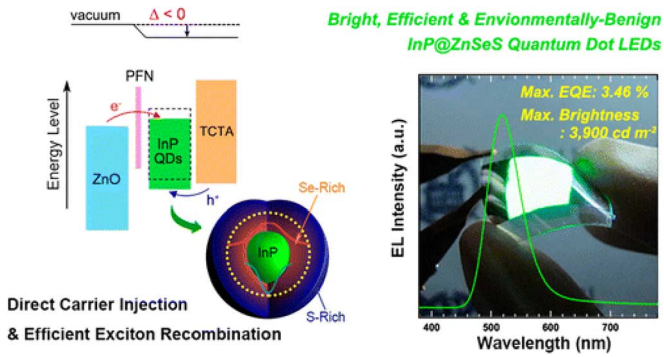

Fig. 30. Cd-free device structure (2013). (Lim *et al.* [38])

ITO, while holes are injected from Al. The HTL materials they used possessed different HOMO energy levels in the range of 5.1–6.0 e.V.

HOMO-LUMO levels are easily determined from solution electrochemistry (viz. cyclic voltammetry) and the absorption edge from UV/VIS absorption spectroscopy of thin films [45]. Kathirgamanthan *et al.* [46] reported absorption, photoluminescence and cyclic voltammetry studies on red and green QDs based on CdSe/ZnS provided by QD Vision.

The red QD's absorption spectra (Fig. 31) of thin films spin coated from a hexane solution showed an edge, which we have attributed to the emissive energy gap in the nanocrystal at $\lambda = 530$ nm and which was at $\lambda = 518$ nm as a thin film. The green QDs showed clear absorption peaks at $\lambda_{\max} = 507.5$ nm (in hexane); 509 nm (thin film). The PL spectra, also shown in Fig. 31, indicate the typical normal distribution type shape. The red QD showed PL emission peaks at $\lambda_{\max} = 627$ nm (thin film); $\lambda_{\max} = 629$ nm (in hexane) and the green at $\lambda_{\max} = 520$ nm (thin film); $\lambda_{\max} = 522$ nm (in hexane).

Cyclic voltammograms (CV) were carried out in acetonitrile (QDs in hexane diluted with acetonitrile) and lithium trifluoromethanesulphonate was used as the supporting electrolyte (Pt foil: working electrode; Pt wire: counter electrode; Ag/AgCl: reference electrode). The CVs for the red QD is given in Fig. 32. Results show quasi reversible oxidation and reduction. We have

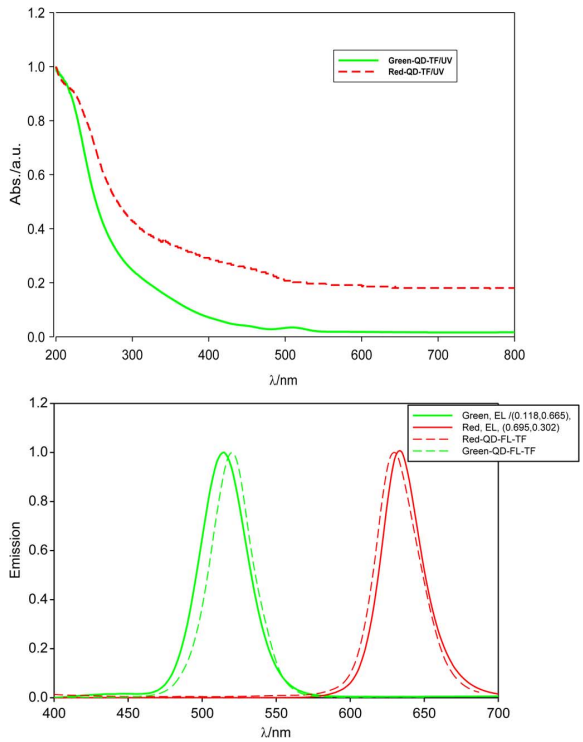

Fig. 31. Absorption spectra of red and green QDs (upper chart) and PL of red and green QDs thin films (lower chart).

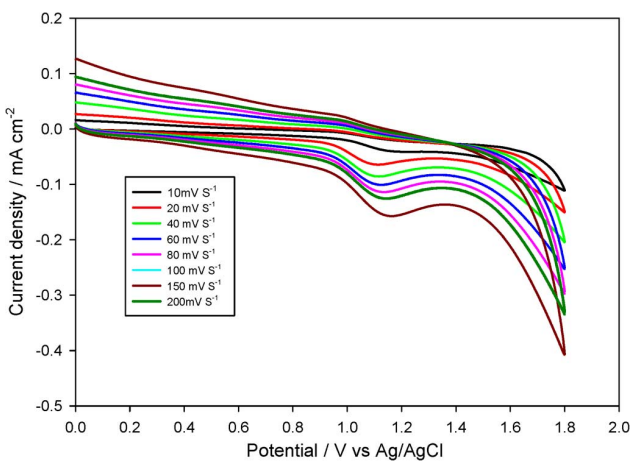

Fig. 32. Cyclic voltammogram showing redox behavior of red QD in CH_3CN with CF_3SO_3Li as the supporting electrolyte.

determined the HOMO level to be set at −5.6 e.V. and the LUMO level at −3.4 e.V. for the red QD.

A clear CV for the green QD could not be obtained as it did not form a stable colloid in the acetonitrile. This is supported by Zeta potential measurements that we carried out. A value of 66.32 mV was obtained for the red QD in acetonitrile indicating excellent stability in solution, but a value of −39.68 mV was obtained for the green QD indicating very poor colloidal stability. We estimated a HOMO level of −5.72 e.V. for the green QD from the CV and a value of −2.41 e.V for its LUMO level from the absorption edge [46].

VI. Conclusion and Future Developments

One of the highest priorities for the commercialization of QLED technology will be to find suitable Cd-free quantum dots. InP-based dots and $CuInS_2$ [44] are already showing much promise in this respect. We have also seen impressive results from devices that use ZnO cores with a MgO shell, indicating that ZnO is also a promising future Cd-free material. In terms of improving performance of QLEDs, there will certainly be much effort directed at optimizing the efficiency of devices. Research by Shen *et al.* [41], for example, has found that as the shell thickness of the quantum dot affects the charge confinement and charge injection in the QD. They recently reported a conventional QD device structure with a power efficiency of 19.7 lm/W for green emission.

As organic hole transporting materials with low HOMO levels (deep HOMO levels) are not readily available (for OLEDs, this is not so), the performance of QLEDs can be further improved by enhancing energy transfer from the hole transport layers into the QD layer through the careful selection of transport materials that can efficiently transfer excitons to QDs via Förster energy transfer [41]. Kim *et al.* [36] have described high-efficiency inverted QLED devices, which are useful for active matrix displays. They deposited two ETL layers, the first Al doped ZnO, followed by a second ETL. A maximum current efficiency of 28.29 cd/A and a power efficiency of 22.11 lm/W was achieved for their stacked ETL inverted green device; an approximately three times improvement on a QLED with a single ETL.

Using materials with high PLs in the red, green, and blue regions of the visible spectrum, Anikeeva *et al.* [43] were able to increase the efficiency of QLEDs four-fold for green devices and by 30% for orange devices. However, they found that there were still challenges in improving the efficiency of blue QLEDs, presumably owing to incomplete energy transfer from organics (weak spectral overlap between the blue QD and the electron and hole transporting materials used). Direct charge injection may also have a higher proportional contribution to the emission from the blue QLED, as manifested in its low EQE value of 0.4%. They suggest this may be remedied by design and synthesis of wide bandgap hole and electron transporting organic materials for improved exciton energy transfer and direct charge injection into blue QDs. Along with continued improvements to luminance and lifetime results for OLEDs and QLEDs, we also expect to see the emergence of "hybrid" devices that incorporate emissive layers using different types of emissive material, for instance a device could contain a blue emitting TADF layer, a green phosphorescent layer and a red QD layer.

Furthermore, we expect to see developments in the OLED lighting arena in the coming years owing to the appealing warm white light that can be created. The saturated colours from QDs, hitherto unattainable from OLEDs, give a technical advantage to QDs. However, the life-times of electroluminescent devices (RGB) are all very short (typically, 100 hours at 1000 cdm^{-2}) and need urgent attention. We have fabricated efficient red and green devices with organic electron injectors and transporters in inverted devices, the results of which will be published elsewhere. We anticipate a great future for quantum dots particularly

if the saturated dark blue (CIE x,y (0.15, 0.03) can be harnessed to give long life-time of at least 10000 hours at 1000 cdm^{-2}.

ACKNOWLEDGMENT

The authors thank QD Vision Inc., Lexington, MA, USA, for the provision of red and green QDs. They also thank Profs J. Buckingham, G. Rodgers, and J. Silver for encouragement.

REFERENCES

[1] G. Destriau, "Researches upon electro-photo-luminescence," *Trans. Faraday Soc.*, vol. 35, pp. 227–233, 1939.
[2] A. Bernanose, M. Comte, and P. Vouaux, "Electroluminescence of organic compounds," *J. Chim. Phys.*, vol. 50, pp. 64–68, 1953.
[3] A. Bernanose, "Electroluminescence of organic compounds," *Brit. J. Appl. Phys.*, vol. 6, pp. S54–S55, Jan. 1955.
[4] W. Helfrich and W. G. Schneider, "Recombination radiation in anthracene crystals," *Phys. Rev. Lett.*, vol. 14, pp. 229–231, Feb. 1965.
[5] N. Holonyak Jr and S. F. Bevacqua, "Coherent (visible) light emission from $Ga(As_{1-x-Px})$ junctions," *Appl. Phys. Lett.*, vol. 1, pp. 82–83, Dec. 1962.
[6] M. G. Craford and F. M. Steranka, "Light emitting diodes," in *Encylopaedia of Applied Physics*, G. L. Trigg, Ed. Weinheim, Germany: Wiley-VCH, 1994, vol. 8, pp. 485–514.
[7] T. Minami, H. Yamada, Y. Kubota, and T. Miyata, "Mn-activated Ca–Ga_2O_3 phosphors for thin-film electroluminescent devices," *Jpn. J. Appl. Phys.*, vol. 36, pp. L1191–L1194, Sep. 1997.
[8] S. Okamoto and E. Nakazawa, "Transient emission mechanisms in thin-film electroluminescent devices with rare-earth-ion-activated SrS phosphor layers," *Jap. J. Appl. Phys.*, vol. 34, pp. 521–526, Feb. 1995.
[9] W. A. Barrow and R. T. Tuenge, "Full color hybrid TFEL display screen," U.S. Patent 4801844 A, 1989.
[10] C. W. Tang and S. A. VanSlyke, "Organic electroluminescent diodes," *Appl. Phys. Lett.*, vol. 51, pp. 913–915, Oct. 1987.
[11] J. M. Burroughes *et al.*, "Light-emitting diodes based on conjugated polymers," *Nature*, vol. 347, pp. 539–541, Oct. 1990.
[12] T. Komoda, "OLED lighting," in *Master Class 3, IDtechEX Conf. Printed Electron.*, Santa Clara, CA, USA, 2014.
[13] R. Xie, D. Battaglia, and X. Peng, "Colloidal InP nanocrystals as efficient emitters covering blue to near-infrared," *J. Amer. Chem. Soc.*, vol. 129, pp. 15432–15433, Nov. 2007.
[14] J. Lim, W. K. Bae, D. Lee, M. K. Nam, J. Jung, C. Lee, K. Char, and S. Lee, "InP@ZnSeS, Core@Composition gradient shell quantum dots with enhanced stability," *Chem. Mater.*, vol. 23, pp. 4459–4463, Sep. 2011.
[15] U. Resch-Genger, M. Grabolle, S. Cavaliere-Jaricot, R. Nitschke, and T. Nann, "Quantum dots versus organic dyes as fluorescent labels," *Nature Meth.*, vol. 5, pp. 763–775, Aug. 2008.
[16] P. O. Anikeeva, C. F. Madigan, S. A. Coe-Sullivan, J. S. Steckel, M. G. Bawendi, and V. Bulović, "Photoluminescence of CdSe/ZnS core/shell quantum dots enhanced by energy transfer from a phosphorescent donor," *Chem. Phys. Lett.*, vol. 424, pp. 120–125, Apr. 2006.
[17] V. Wood and V. Bulović, "Colloidal quantum dot light-emitting devices," *Nano Rev.*, vol. 1, pp. 5202–5208, Jul. 2010.
[18] B. S. Mashford *et al.*, "High-efficiency quantum-dot light-emitting devices with enhanced charge injection," *Nature Photon.*, vol. 7, pp. 407–412, Apr. 2013.
[19] J. Zhao *et al.*, "Efficient CdSe/CdS quantum dot light-emitting diodes using a thermally polymerized hole transport layer," *Nano. Lett.*, vol. 6, pp. 463–467, Feb. 2006.
[20] H. M. Haverinen, R. A. Myllylä, and G. E. Jabbour, "Inkjet printed RGB quantum dot-hybrid LED," *J. Display Technol.*, vol. 6, no. 3, pp. 87–89, Mar. 2010.
[21] J. S. Steckel *et al.*, "Color-saturated green-emitting QD-LEDs," *Angwe. Chem. Int. Ed.*, vol. 45, pp. 5796–5799, Jul. 2006.
[22] D. Bera, L. Qian, and P. H. Holloway, *Luminescent Materials and Applications*, A. Kitai, Ed. Hoboken, NJ, USA: Wiley, 2008, pp. 19–65.
[23] X. B. Chen, Y. B. Lou, A. C. Samia, and C. Burda, "Coherency strain effects on the optical response of core/shell heteronanostructures," *Nano Lett.*, vol. 3, pp. 799–803, 2003.
[24] M. Grabolle, J. Ziegler, A. Merkulor, T. Nann, and U. Resch-Genger, "Stability and fluorescence quantum yield of CdSe-ZnS quantum dots—Influence of the thickness of the ZnS shell," *Ann. New York Acad. Sci.* , vol. 1130, pp. 235–241, May 2008.
[25] J. Gilbertson and T. Davis, "Colloidal CdSe quantum dot electroluminescence: Ligands and light-emitting diodes," *Microchim. Acta*, vol. 160, pp. 345–350, Jun. 2007.
[26] B. Ludolph, M. A. Malik, P. O'Brien, and N. Revaprasadu, "Novel single molecule precursor routes for the direct synthesis of highly monodispersed quantum dots of cadmium or zinc sulfide or selenide," *Chem. Commun.*, vol. 17, pp. 1849–1850, 1998.
[27] M. Green, "The Nature of Quantum Dot Capping Ligands," *J. Mater. Chem.*, vol. 20, pp. 5797–5809, Apr. 2010.
[28] C. B. Murray, D. J. Norris, and M. G. Bawendi, "Synthesis and characterisation of nearly monodisperse CdE (E = S, Se, Te) semiconductor nanocrystallites," *J. Amer. Chem. Soc.*, vol. 115, pp. 8706–8715, Sep. 1993.
[29] V. Wood, M. J. Panzer, J. E. Halpert, J.-M. Caruge, M. G. Bawendi, and V. Bulović, "Selection of metal oxide charge transport layers for colloidal quantum dot LEDs," *ACS Nano*, vol. 3, pp. 3581–3586, Nov. 2009.
[30] D. Y. Kondakov, T. D. Pawlik, T. K. Hatwat, and J. P. Spindler, "Triplet annihilation exceeding spin statistical limit in highly efficient fluorescent organic light-emitting diodes," *J. Appl. Phys.*, vol. 106, pp. 124510–124517, Dec. 2009.
[31] F. B. Dias *et al.*, "Triplet harvesting with 100% efficiency by way of thermally activated delayed fluorescence in charge transfer OLED emitters," *Adv. Mater.*, vol. 25, pp. 3707–3714, May 2013.
[32] H. Uoyama, K. Goushi, K. Shizu, H. Nomura, and C. Adachi, "Highly efficient organic light-emitting diodes from delayed fluorescence," *Nature*, vol. 492, pp. 234–238, Nov. 2012.
[33] T. Tsujimura, *OLED Displays: Fundamentals and Applications*. Hoboken, NJ, USA: Wiley-SID Series, 2012.
[34] D. Gerion *et al.*, "Synthesis and properties of biocompatible water-soluble silica-coated CdSe/ZnS semiconductor quantum dots," *J. Phys. Chem. B*, vol. 105, pp. 8861–8871, Jun. 2001.
[35] B. S Mashford, M. Stevenson, Z. Popovic, C. Hamilton, Z. Zhou, C. Breen, J. Steckel, V. Bulovic, M. Bawendi, S. Coe-Sullivan, and P. T. Kazlas, "High-efficiency quantum-dot light-emitting devices with enhanced charge injection," *Nature Photon.*, vol. 7, pp. 407–412, Apr. 2013.
[36] H.-M. Kim and J. Jang, "High-efficiency inverted quantum-dot light emitting diodes for display," in *SID 2014 Symp. Dig. Tech. Papers*, 2014, vol. 45, pp. 67–70.
[37] K. Qasim, J. Chen, W. Lei, Z. Li, J. Pan, Q. Li, J. Xia, and Y. Tu, "Influence of layer thickness on the performance of quantum dots light emitting devices," in *SID 2014 Symp. Dig. Tech. Papers*, vol. 45, pp. 63–66.
[38] J. Lim, W. K. Bae, J. Kwak, S. Lee, C. Lee, C. Lee, and K. Char, "Perspective on synthesis, device structures, and printing processes for quantum dot displays," *Opt. Mater. Express*, vol. 2, pp. 594–628, May 2012.
[39] J. Lim *et al.*, "Highly efficient cadmium-free quantum dot light-emitting diodes enabled by the direct formation of excitons within InP@ZnSeS quantum dots," *ACS Nano*, vol. 7, pp. 9019–9206, Oct. 2013.
[40] J. Kwak *et al.*, "Bright and efficient full-color colloidal quantum dot light-emitting diodes using an inverted device structure," *Nano Lett.*, vol. 12, pp. 2362–2366, Apr. 2012.
[41] H. Shen *et al.*, "Efficient and bright colloidal quantum dot light-emitting diodes via controlling the shell thickness of quantum dots," *ACS Appl. Mater. Interfaces*, vol. 5, pp. 12011–12016, Nov. 2013.
[42] P. O. Anikeeva, C. F. Madigan, S. A. Coe-Sullivan, J. S. Steckel, M. G. Bawendi, and V. Bulović, "Photoluminescence of CdSe/ZnS core/shell quantum dots enhanced by energy transfer from a phosphorescent donor," *Chem. Phys. Lett.*, vol. 424, p. 120, Apr. 2006.
[43] P. O. Anikeeva, J. E. Halpert, M. G. Bagwendi, and V. Bulović, "Quantum dot light-emitting devices with electroluminescence tunable over the entire visible spectrum," *Nano Lett.*, vol. 9, pp. 2532–2536, Jun. 2009.
[44] B. Chen *et al.*, "Highly emissive and colour tunable $CuInS_2$-based colloidal semiconductor nanocrystals: Off stoichiometry effects and improved electroluminescence performance," *Adv. Functional Mater.*, vol. 22, pp. 2081–2088, Mar. 2012.
[45] P. Kathirgamanathan *et al.*, "Discovery of two new phases of zirconium tetrakis(8-hydroxyquinolinolate): Synthesiscrystal structure and their electron transporting characteristics in organic light emitting diodes (OLEDs)," *J. Mater. Chem.*, vol. 21, pp. 1762–1771, 2011.
[46] P. Kathirgamanathan, L. Bushby, M. Kumarverl, S. Ravichandran, and S. Surendrakumar, "Red and green quantum dot based LEDs demonstrating excellent color coordinates," in *SID Conf. Proc.*, 2015.

Poopathy Kathirgamanathan received the Ph.D. degree from Exeter University, Devon, U.K., in 1980.

He is a Professor of Electronic Materials Engineering, Wolfson Centre, Brunel University, U.K., and is one of the worlds leading experts in Organic Electronics. Following the Ph.D. degree from Exeter (Sir Arthur Reed Scholar), he pioneered research and development in the area of Organic Electronics at Newcastle University, Cookson Group plc., University College London, and London South Bank University (Chair in Electronic Materials Engineering since 1993). In 2000, he founded OLED-T, based on the technology that he developed at London South Bank University and served as the CTO of OLED-T until the company and most of the I.P. (48 patents) of OLED-T was sold to Merck Chemicals, Germany, in August 2008. He moved to Brunel University, Uxbridge, U.K., in March 2009, where he continues to develop new materials for OLEDs, QLEDs, OPV, and OTFT, in addition to electrochemistry and nanotechnology. He is passionate about the commercialization of OLEDs for displays and lighting and OPV (Organic PV). He has received a total of GB £2.1 million pounds from Royal Society, TSB, EU, and industrial funding over the last three years. He has over 200 publications and patents, and over 150 conference papers.

Prof. Kathirgamanathan is currently an Executive Committee Member of the Materials Chemistry Group, Society of Chemical Industries, London, U.K., and also served as the Chairman of the Group from 1999 to 2000. He is also a Committee Member of the Materials Chemistry Division (RSC) since July 2013, and the Regional Vice President, Europe, Society for Information Displays, since May 2013. He was a recipient of prestigious Sir Monty Finniston Award in recognition of his achievements in developing electroactive and light emitting materials and winner of awards for the best R&D in OLED's in 2006 and 2007 at the Organic Semiconductor Conference (Frankfurt, Germany). He is an Associate Editor of the IEEE/OSA JOURNAL OF DISPLAY TECHNOLOGY since 2012. He was recently awarded GB £4 million by EC to develop flexible OLED lighting. He has been a Fellow of the Royal Society of Chemistry since 1992, and of the Institute of Physics since 1994

Lisa M. Bushby, photograph and biography not available at time of publication.

Muttulingam Kumaraverl, photograph and biography not available at time of publication.

Seenivasagam Ravichandran, photograph and biography not available at time of publication.

Sivagnanasundram Surendrakumar, photograph and biography not available at time of publication.